Development 137, 1965-1973 (2010) doi:10.1242/dev.049080

Drosophila adult muscle precursors form a network of interconnected cells and are specified by the *rhomboid*-triggered EGF pathway

Nicolas Figeac, Teresa Jagla, Rajaguru Aradhya, Jean Philippe Da Ponte and Krzysztof Jagla*

SUMMARY

In *Drosophila*, a population of muscle-committed stem-like cells called adult muscle precursors (AMPs) keeps an undifferentiated and quiescent state during embryonic life. The embryonic AMPs are at the origin of all adult fly muscles and, as we demonstrate here, they express repressors of myogenic differentiation and targets of the Notch pathway known to be involved in muscle cell stemness. By targeting GFP to the AMP cell membranes, we show that AMPs are tightly associated with the peripheral nervous system and with a subset of differentiated muscles. They send long cellular processes running along the peripheral nerves and, by the end of embryogenesis, form a network of interconnected cells. Based on evidence from laser ablation experiments, the main role of these cellular extensions is to maintain correct spatial positioning of AMPs. To gain insights into mechanisms that lead to AMP cell specification, we performed a gain-of-function screen with a special focus on lateral AMPs expressing the homeobox gene *ladybird*. Our data show that the *rhomboid*-triggered EGF signalling pathway controls both the specification and the subsequent maintenance of AMP cells. This finding is supported by the identification of EGF-secreting cells in the lateral domain and the EGF-dependent regulatory modules that drive expression of the *ladybird* gene in lateral AMPs. Taken together, our results reveal an unsuspected capacity of embryonic AMPs to form a cell network, and shed light on the mechanisms governing their specification and maintenance.

KEY WORDS: AMP, Stem cell, Muscle, *Drosophila*, Ladybird

INTRODUCTION

Several populations of stem cells have been identified in the fruit fly over the last few years (for a review, see Pearson et al., 2009). Studies on *Drosophila* germline stem cells (GSCs) (Spradling et al., 2001) and, more recently, intestinal stem cells (ISCs) (Micchelli and Perrimon, 2006; Ohlstein and Spradling, 2006; Takashima et al., 2008) that persist in adult flies have helped establish niche models of stem cell self-renewal. Conversely, during development, populations of transient stem cells play crucial roles in the formation of specific tissues (Pearson et al., 2009). For example, transient populations of neural stem cells called neuroblasts undergo a series of asymmetric cell divisions that ensure self-renewal and at the same time give rise to a large range of neural lineages that undergo differentiation (Yu et al., 2006). In the embryonic mesoderm, muscle progenitor cells were shown to divide asymmetrically like the neuroblasts (Ruiz Gomez et al., 1997), but unlike neuroblasts, they divide only once, and give rise either to two distinct muscle founder cells that enter the differentiation process or to a muscle founder and a cell called an adult muscle precursor (AMP) that keeps an undifferentiated state (Ruiz Gomez et al., 1997; Figeac et al., 2007). As the AMPs express markers specific to muscle progenitors, such as the b-HLH transcription factor Twist (Bate et al., 1991; Figeac et al., 2007), the asymmetric cell division leading to the production of an AMP resembles the asymmetric cell division of the neuroblasts that ensure self-renewal. The key role of AMP cells in adult muscle growth and in the regeneration of a subset of thoracic muscles also indicates that the AMPs share properties with vertebrate satellite cells (Maqbool and Jagla, 2007). Thus, the AMPs emerge as a novel, muscle-committed population of transient *Drosophila* stem cells. Based on this assumption, we aimed to gain insights into AMP cell behaviour and the genetic control of their specification to improve our knowledge on muscle stem cells in general. To address these issues, we first attempted to identify new cell markers capable of tracking AMPs during development. We found that two targets of Notch signalling, E(spl)M6 and Him, as well as two transcription factors, Zfh1 and Cut, are specifically expressed in *Drosophila* AMPs. Both Him (Liotta et al., 2007) and Zfh1 (Postigo et al., 1999) are able to counteract Mef2-driven myogenic differentiation, probably acting as Mef2 repressors, whereas Cut is known to play a role in the diversification of flight muscles (Sudarsan et al., 2001) and to act as a neural selector gene (Bodmer et al., 1987). The AMP-specific roles of these genes have not yet been investigated. Using the Notch-responsive element of E(spl)M6 to drive membrane-targeted GFP in the AMPs, we observed that AMPs send long cellular processes and are interconnected. We also designed a genetic screen to identify genes affecting AMP cell pattern and found that *rhomboid* (*rho*) and other EGF pathway components control AMP specification and subsequently protect them against apoptosis. A key role for EGFR signalling was further supported by the identification of EGF-secreting cells that ensure AMP cell maintenance and by the finding that regulatory modules driving expression in lateral AMPs carry functional EGF (ETS)-responsive motifs.

GReD, INSERM U931, CNRS UMR6247, Clermont University, Faculté de Médecine, 28 Place Henri Dunant, Clermont-Ferrand, 63000, France.

*Author for correspondence (christophe.jagla@u-clermont1.fr)

Accepted 18 April 2010

MATERIALS AND METHODS

Drosophila stocks

The M6-GFP (Rebeiz et al., 2002), Hid A329 (Bergmann et al., 2002) and UAS-Lb (Jagla et al., 1998) lines have been previously described. The collection of EP gain-of-function lines, including the EP3704 (*rho*) line, was provided by Szeged Stock Center. UAS-EGFRDN (BL5364), UAS-Htl (BL5367), UAS-pointed1 (BL869), UAS-GAP-GFP (BL4522), 69BGAL4 (BL1774) and mutant alleles for *Star* (BL2772), *spitz* (BL1859), *yan* (BL3101) and H99 apoptosis inducers (BL1576) were kindly provided by Bloomington Stock Center. Duf-GAL4 and Duf-*lacZ* lines were from K. Vijay Raghavan (NCBS, Bangalore, India). An M6-GAL4 driver line was generated in-lab as follows. A 5′ region of *E(spl)m6* gene from –2098 to +37, corresponding to the region previously used to drive GFP expression in the M6-GFP construct (Rebeiz et al., 2002), was amplified using the following primers: forward, ATATCTAGACGACGCTTA-TTATCAGCCCAA and reverse, ATAGGATCCGAGTTCTTAGC-GCGTTGATTC. The resulting 2135 bp PCR product directionally cloned (*Xba*I/*Bam*HI) into pPTGAL vector (Sharma et al., 2002) was injected into w^{1118} embryos to produce transgenic lines.

Antibodies and RNA probes

Wholemount embryos were stained using the following primary antibodies: anti-Twi (rabbit, 1/300, made in-lab; see below), anti-Twi (guinea pig, 1/300) from E. Furlong (European Molecular Biology Laboratory, Heidelberg, Germany), anti-Twi (rabbit, 1/300) from S. Roth (Cologne University, Germany), anti-b3 Tubulin (rabbit, 1/2000) from R. Renkawitz-Pohl (Friedrich-Alexander University of Erlangen-Nuremberg, Erlangen, Germany), anti-Mef2 (rabbit, 1/1000) from H. Nguyen (Friedrich-Alexander University of Erlangen-Nuremberg, Erlangen, Germany), anti-Kr (guinea pig, 1/800) from M. Frasch (Friedrich-Alexander University of Erlangen-Nuremberg, Erlangen, Germany), anti-Zfh1 (rabbit, 1/500) from R. Bodmer (The Burnham Institute for Medical Science, La Jolla, CA, USA) and anti-Lbe (mouse, 1/2500) (Jagla et al., 1998). We also used mouse monoclonal anti-Elav (1/500) and anti-Cut (1/200) from DSHB, anti-DpERK (mouse, 1/100) and anti-LacZ (goat, 1/1000) from Sigma, and anti-GFP (goat 1/300) from Biogenesis. Secondary antibodies coupled to CY3, CY5, FITC or Alexa488 were obtained from Jackson ImmunoResearch, and TSA-fluorescein was obtained from PerkinElmer.

Fluorescent in situ hybridization was performed according to Nagaso et al. (Nagaso et al., 2001) using previously described Dig-labelled RNA probes for *Him* (19) and *rho* (22). A Zeiss LSM510 microscope was used for confocal imaging with Volocity software for image analysis and 3D movie generation. Polyclonal antibodies were generated against the N-terminal part of the Twist protein encoded by the first exon. We used the following pair of primers to generate the expression vector: forward, ATAGAGCTCGAGCGCTCGCTCGGTGTCG and reverse, ATAGGTA-CCTGTGGGAGTTTGAGGGTCTG. The 1215 bp PCR product digested with *Sac*I and *Kpn*I was cloned in-frame into pRSET B His-tagged vector (Invitrogen). His-Twi fusion protein was purified using NI-NTA agarose (Qiagen). Antibody was then generated in rabbit by Proteogenix SA and purified on an affinity column carrying recombinant Twi protein.

Time-lapse and laser ablation experiments

Age-matched M6-GAL4; UAS-GAP-GFP embryos were dechorionated, aligned laterally on long coverslips and used for time-lapse experiments on a Leica MP-SP5 RS inverted confocal microscope. Images were taken every 5 minutes over a 3-6 hour period and converted into 4D files using Imaris Suite (Bitplane). The multiphoton point ablation device available on the Leica MP-SP5 confocal microscope was used to destroy connections between the AMPs. Three independent ablation experiments were performed and analyzed on stage-14 and stage-15 embryos. We applied the following IR laser settings: wavelength, 920 nm; time, 20 ms; gain, 80%; offset, 50%. Post-ablation time-lapse movies were generated as the wild-type movies.

LME and LAMPE regulatory regions and site-specific mutagenesis

LME (*ladybird muscle enhancer*)-*lacZ* transgenic lines were generated by PCR amplification of a 563 bp fragment with primers ATAGGTAC-CTTCATAAGCCAAATGTATCGGC (forward) and ATATCTAGA-CACAGATTCTCCTTCTTCTTTC (reverse) carrying *Kpn*I and *Xba*I restriction sites, respectively, then directionally cloned into a PWHSPLAC vector. In a similar manner, *LAMPE* (*lateral adult muscle precursor enhancer*)-*lacZ* lines were generated by cloning a 156 bp genomic fragment amplified with ATATCTAGATCTTTGACCAAAG-CAAGTCC (forward) and ATAGGTACCCGCGGAAGCAAT-AAAATCTC (reverse) primers. Site-specific mutagenesis was performed to produce transgenic lines carrying LME and LAMPE regions with mutated Mef2, ETS and Lb binding sites. The following TF binding sites were found within the *LME* and *LAMPE* sequences and a mutated version of each site, generated by PCR site-specific mutagenesis, is specified (mutated nucleotides are in bold): wild-type Mef2 (Junion et al., 2005), CTCATAAATAG; mutated Mef2, CTC**CCGG**ATAG; wild-type Lb (Junion et al., 2007), VYTAAYHA; mutated Lb, VYT**SS**YHA; wild-type ETS1, aCMGGAWGt; mutated ETS1, aCAG**AGCAg**; wild-type ETS2, gCWTCCKCg; mutated ETS2, **tAGAT**CGCg. V=G/C/A; Y=T/C; H=A/C/T; S=C/G; M=A/C; W=A/T; K=T/G. At least three independent transgenic lines were generated and analyzed for each genetic context.

RESULTS

Notch targets and repressors of myogenic differentiation are expressed in AMPs

In late *Drosophila* embryos, each abdominal hemisegment features six AMPs at stereotypical positions associated with differentiating muscle fibres (Fig. 1A-C,K). To better characterize these cells, we first tested whether the Notch pathway, which is known to be required for generation of satellite cells from muscle progenitors (Vasyutina et al., 2007) and for keeping them ready to engage in muscle regeneration (Carlson et al., 2008), is also active in AMPs. Analysis of a GFP reporter line, M6-GFP, described as a read-out of the Notch pathway in *Drosophila* (Lai et al., 2000), revealed that it is co-expressed with Twist in AMPs (Fig. 1D). Also, transcripts of another Notch target, *Him* (Rebeiz et al., 2002; Liotta et al., 2007), specifically accumulated in AMPs (Fig. 1G). By testing several mesodermal cell markers, we found that, in addition to Twist, two other transcription factors, Zfh1 and Cut, are expressed in all AMPs (Fig. 1F,H). *Zfh1* expression in embryonic AMPs has also been reported by Sellin et al. (Sellin et al., 2009), whereas *cut* has previously been used to reveal a subset of AMPs associated with larval wing (Sudarsan et al., 2001) and leg imaginal discs (Soler et al., 2006). Despite expressing common markers, the AMPs are heterogenous and differ by the expression of muscle identity genes (Fig. 1K). For example, *slouch* (*S59*) and *Pox meso* are specifically expressed in ventral (V) AMPs (Knirr et al., 1999; Duan et al., 2007) whereas *ladybird* (*lb*) and *Kruppel* (*Kr*) display lateral (L) AMP-specific expression (Fig. 1I-K).

Embryonic AMPs are interconnected and form a cell network

To gain insights into AMP cell shapes and their behaviour, we generated an M6-GAL4 line that recapitulates M6-GFP expression (compare Fig. 1D with 1E) and used it to drive a membrane-targeted GFP. It has been previously reported that AMPs are associated with the larval peripheral nervous system (PNS) and that in *daughterless* mutant embryos lacking all the larval sensory system, the final pattern of AMPs is deranged (Bate et al., 1991). Here, we show (Fig. 1L,N,O; see Movie 1 in the supplementary material) that all embryonic AMPs are closely associated with both the PNS and the differentiated muscles, sitting either at the top of muscle fibres [LAMPs and dorsal (D)

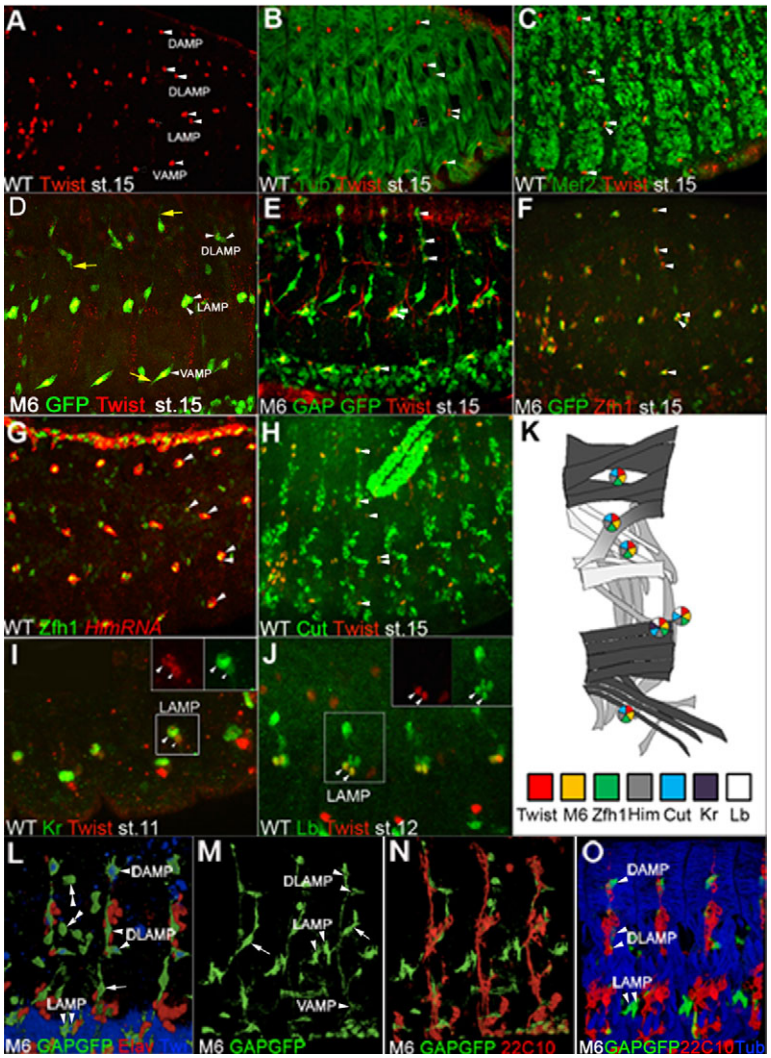

Fig. 1. Markers of embryonic AMP cells. (**A-C**) Lateral views of stage-15 embryos stained with anti-Twi antibody to reveal AMP patterns. (A) Wild type. (B,C) Embryos were co-stained with anti-β3-Tubulin to reveal muscle fibres (B) or anti-Dmef2 (C) to reveal muscle nuclei. Arrowheads point to AMP cells located ventrally (VAMP), laterally (LAMP), dorsolaterally (DLAMP) and dorsally (DAMP). (**D**) Notch-responsive element from the *E(spl)m6* gene drives GFP expression in Twi-positive AMPs (arrowheads). Yellow arrows point to cytoplasmic extensions of AMP cells. (**E**) Membrane-targeted GFP expression driven by an *E(spl)m6* element reveals that AMPs send long processes in a dorsoventral direction and are interconnected (arrowheads). (**F**,**G**) Repressors of myogenic differentiation *Zfh1* (F) and *Him* (G) are expressed in AMPs (arrowheads). (**H**) Homeobox selector gene *cut* marks AMPs (arrowheads). (**I**,**J**) Differential expression of Kruppel (Kr) in one of two LAMPs (arrow), which are both Lb-positive and Twi-positive. Insets at right corner of (I) show a high Kr expression in the more anterior LAMP (arrow) compared with a weak Kr expression in the posterior LAMP (arrowhead). Both LAMPs are Lb and Twi positives (see insets in J). (**K**) A scheme illustrating the location of AMPs within a hemisegment and a code of differential gene expression. (**L-O**) Snapshots from 3D reconstructions of GAP-GFP reveal AMPs (arrowheads). (L) Nuclei of PNS neurons lie close to the AMP extensions. The arrow points to M6-GFP-positive and Twist-negative AMP-like cells connecting LAMPs with DLAMPs. M6-GAP-GFP staining also reveals a group of Twist-negative and Elav-negative cells displaying a more regular morphology (double arrowhead; also see Fig. S3 in the supplementary material). (M) Interconnections of AMPs at the end of embryogenesis and their alignment (N) with the intersegmental nerves of the PNS. Arrows show AMP-like cells. (O) General view of AMPs, PNS and body wall muscles.

AMPs] or on their internal face [dorsolateral (DL) AMPs and VAMPs)]. We demonstrate that, in late embryos, the AMPs form a network of cells displaying irregular shapes and that are interconnected by long cellular processes aligning PNS nerves (Fig. 1L-O; see Movies 1-3 in the supplementary material). Connections between the AMPs initially form within the parasegments, but the AMPs very quickly send filopodia posteriorly and make contact with DLAMPs of the adjacent segment, thus interlinking all AMPs. In addition to the interconnected M6+/twi+ AMPs, we also identified a population of morphologically distinct M6+/twi– cells of unknown fate, located more internally in central and posterior regions of the abdomen (Fig. 1L; see Movie 1 in the supplementary material).

To understand how the network of AMPs is formed during embryonic development, we performed a series of time-lapse experiments. Our data show (Fig. 2A-E; see Movie 4 in the supplementary material) that, starting from early stage 14, VAMPs send two main filopodia dorsally, one growing along the intersegmental nerve and targeting DAMPs and another one that follows the segmental nerve in the direction of LAMPs. As a result, by the end of stage 15, within each abdominal segment the VAMPs become connected to LAMPs as well as DLAMPs and DAMPs (see Movie 4 in the supplementary material). Interestingly, the LAMPs of a given segment also make contact with the major ventral-dorsal extension of the adjacent posterior segment. They do so via an intermediary M6-positive cell that is *twi*-negative (Fig. 1M; Fig. 2D,E) so that, at the end of embryogenesis, all AMPs are interconnected. As these connections are no longer seen in the second instar larvae when the AMPs start to proliferate and migrate to different locations (Farell and Keshishian, 1999) (data not shown), we hypothesize that they might play a role in spatially positioning AMPs and/or keeping them quiescent.

To investigate the role of the interconnections, we used multiphoton laser ablation to analyze AMP cell behaviour in embryos in which the main ventral-dorsal extensions were disrupted. Our time-lapse experiments (Fig. 2F-J; see Movie 5 in the supplementary material) clearly show that the AMPs disconnected by ablation from the AMP cell network become highly mobile and are no longer detected at their stereotypical locations. They move randomly and fail to re-establish contacts with other AMPs (Fig. 2I,J; see Movie 5 in the supplementary material). In embryos ablated at a late stage of development (after stage 15), when the cellular connections are already completely formed, the AMPs send cellular processes laterally and contact AMPs from adjacent segments (data not shown). This allows them to keep an approximately correct dorsoventral position. Interestingly, ablation at stage 14, when the AMP cells are not yet interconnected, leads to the disruption of the AMP cell network and

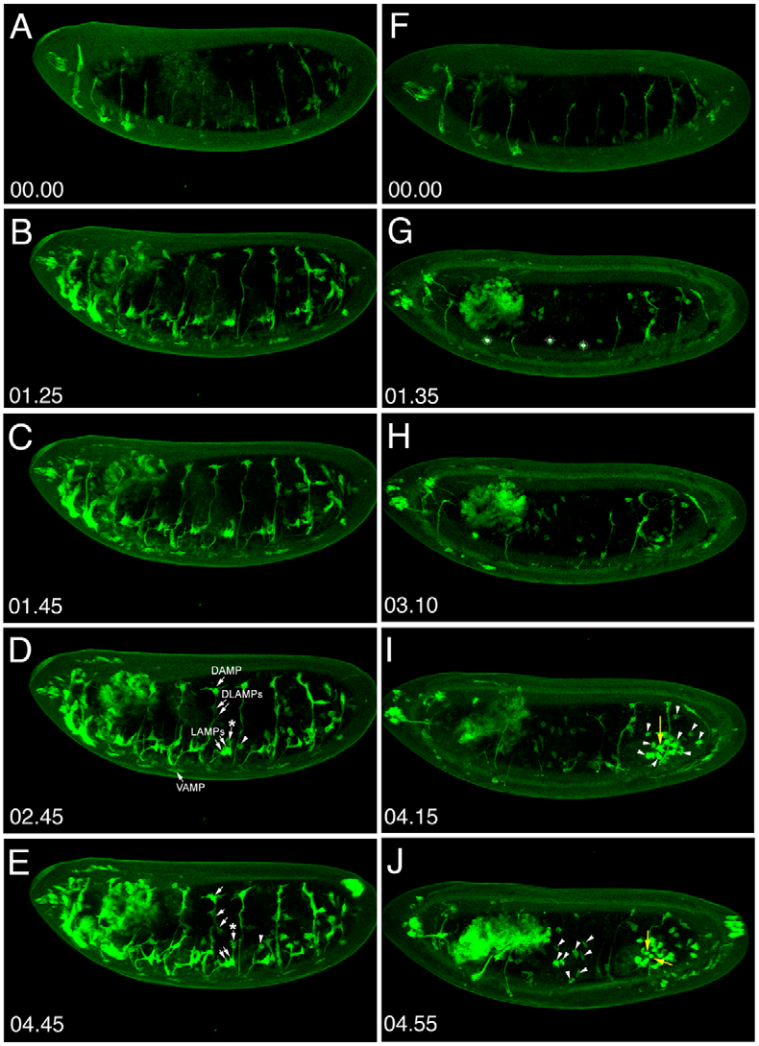

Fig. 2. Formation of the AMP cell network during embryogenesis and behaviour of AMP cells separated from the network by laser ablation. (**A-E**) Selected time-point views from Movie 4 in the supplementary material and (**F-J**) selected time-point views from the Movie 5 in the supplementary material. Panels show dorsolateral views of developing wild-type M6-GAL4; UAS-GAP-GFP embryos (A-E) or embryos in which connections between LAMPs and DLAMPs in three abdominal segments were disrupted by laser ablation (F-J). The first time-points (A,F) correspond to stage 14 of embryogenesis. AMP cells are indicated by arrows (D,E). Asterisks in D and E point to intermediary M6-positive cells that make connections between LAMPs and the ventral-dorsal extension of the posterior segment. Moving, non-connected M6-positive cells are indicated by the arrowheads in D and E. Ablation points are indicated by target symbols (G). The embryo shown in F-J was ablated at stage 14 at the time the ventral-dorsal extensions are still growing dorsally, when AMP cells are not yet interconnected. This led to disruption of the AMP network. Compared with non-ablated embryos (D,E), an increased number of free M6-GFP cells of rounded morphology is seen 4-5 hours after ablation (arrowheads in I,J). Notice that the adjacent non-ablated segments are also affected. The yellow arrow in I points to a dividing M6-positive cell, which gives rise to two rounded cells indicated by yellow arrows in J (also see Movie 5 in the supplementary material).

to an increased number of free M6-GFP cells of rounded morphology, some of which undergo mitosis (yellow arrows, Fig. 2I,J; see Movie 5 in the supplementary material).

Thus, we conclude that the one important reason for which AMPs are interconnected is to ensure their precise spatial positioning. As in certain ablation conditions we observe supernumerary free M6-positive cells undergoing cellular division, we believe that formation of a network promotes the quiescent state of AMPs.

Dual role of the EGFR pathway in specification and maintenance of AMPs

Based on the premise that AMPs represent a novel population of transient *Drosophila* stem cells, we performed a gain-of-function screen to identify genes affecting their specification. This was done using a previously described collection of EP lines (Bidet et al., 2003) and two of the AMP markers, i.e. Twi to reveal all AMPs and Lb to specifically visualize LAMPs. Among the identified candidates affecting the number of AMPs, we found that the pan-mesodermal overexpression of *rho*, required for maturation of EGFR ligand Spitz (Fig. 3I), leads to the specification of a much higher number of AMPs (Fig. 3B; Table 1). Interestingly, AMPs are only overproduced in the dorsal, dorsolateral and lateral regions, reflecting the specificity of their response to EGFR signalling. The promoter effect of the EGFR pathway is supported by the specification of supernumerary AMPs in embryos expressing a constitutively active form of EGFR (EGFCA) in the mesoderm (Fig. 3C; Table 1) and a loss of the majority of AMPs when a dominant-negative form of EGFR (EGFRDN) was overexpressed (Fig. 3F; Table 1). Loss-of-function mutations of *spitz*, which encodes an EGFR ligand, and *Star*, which is required for targeting Spitz to the Golgi, result in an EGFRDN-like phenotype (Fig. 3D,E; Table 1). Here again, only the DAMPs, DLAMPs and LAMPs are affected, while the number of VAMPs remains unchanged (Fig. 3C-F; Table 1). Moreover, we observed that the pan-mesodermal expression of the constitutively active form of RAS leads to a phenotype resembling that of EGFRCA (Table 1; see Fig. S1 in the supplementary material), which strongly suggests that the signal transduced by EGFR has a major impact on RAS-dependent AMP specification. This assumption is further supported by the minor changes in AMP cell number in embryos expressing the constitutively active fibroblast growth factor (FGF) receptor Heartless (see Fig. S1 in the supplementary material).

As discussed previously, AMPs arise from a subset of muscle progenitors, which segregate from a group of cells called promuscular clusters. It is thought that non-segregating cells from promuscular clusters give rise to fusion-competent myoblasts, but

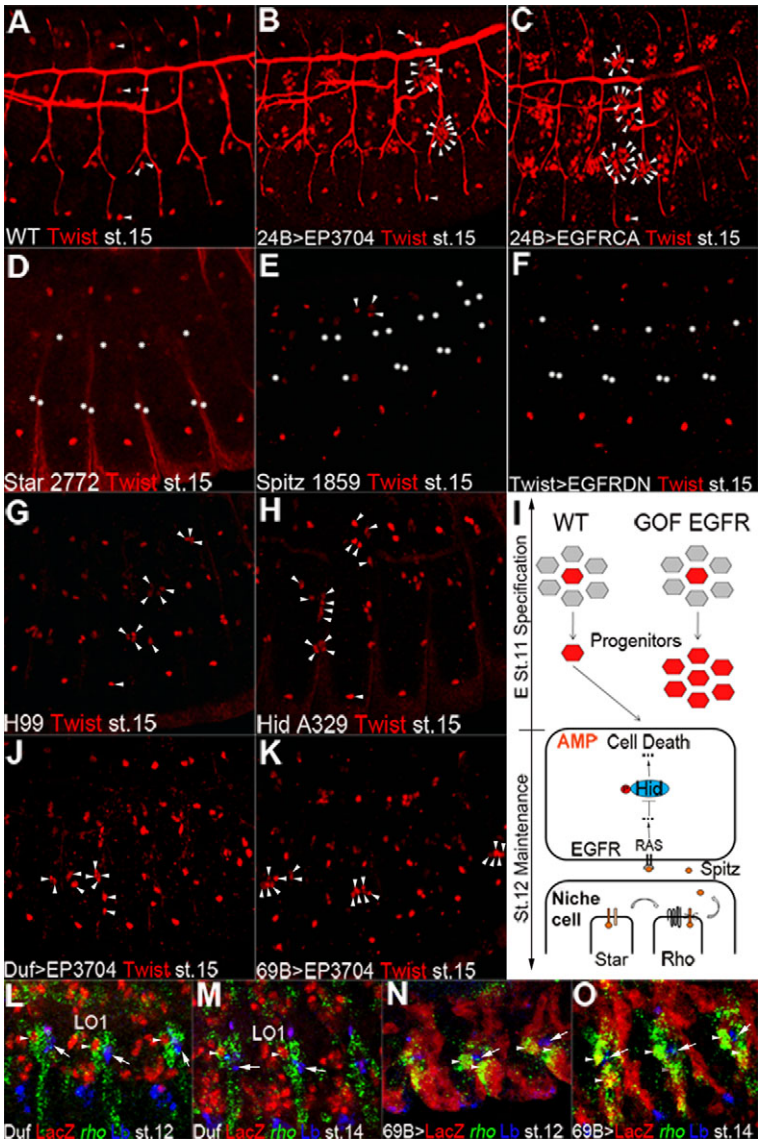

Fig. 3. EGFR pathway components regulate specification and maintenance of AMPs. (**A-I**) AMP pattern revealed using anti-Twi antibody. (A) Wild type. (B,C) Pan-mesodermal expression of *rho* (B) and a constitutively active form of EGFR (C) leads to a strong increase in the number of AMPs at lateral, dorsolateral and dorsal positions. Background staining in the tracheal system seen in A-C is due to a different anti-Twi antibody originating from F. Perrin-Schmidt (IGBMC, Strasbourg). Notice that VAMPs are unaffected. The number of LAMPs, DLAMPs and DAMPs is dramatically reduced in embryos with affected processing of EGF ligand (D), lacking the ligand (E) or expressing a dominant-negative form of EGFR (F). Arrowheads point to AMPs, whereas asterisks indicate their loss. (G,H) Blocking apoptosis by deleting all inducers of apoptosis (G) or by specific mutation of Hid (H) results in a moderately increased number of AMPs (arrowheads). (I) Scheme illustrating the anti-apoptotic role of EGFR. (**J**,**K**) The supernumerary AMPs are generated in embryos in which late mesodermal (J) or epidermal (K) gain-of-function of *rho* is induced, suggesting that EGF signalling plays a dual role and, in later stages, is involved in AMP survival. (**L-O**) The anti-apoptotic function of EGF is supported by specific expression of *rho* in Duf-positive LO1 founder (arrowheads in L,M) and 69B-positive epidermal cells (arrowheads in N,O) overlying the LAMPs (arrows).

the developmental destination of non-segregating cells from the promuscular clusters that give rise to AMPs is unknown. To investigate this issue, we tested whether they are eliminated by apoptosis. A few supplementary AMPs per hemisegment were observed in embryos with impaired apoptosis (Fig. 3G), thus supporting a view that non-segregating cells can adopt AMP-like fate and become eliminated by apoptotic events. Interestingly, the analysis of the mutants deficient in three *Drosophila* activators of apoptosis, i.e. *reaper*, *grim* and *Hid* (*W*, *Wrinkled* – FlyBase), showed that LAMPs, DLAMPs and DAMPs were overproduced (Fig. 3G), whereas VAMP numbers remained unchanged, highlighting a phenotype reminiscent of that observed in the EGFR gain-of-function situation (Fig. 3B,C). As the EGFR pathway is known to protect cells from apoptosis by repressing Hid (Bergmann et al., 2002), we investigated whether AMP number is regulated by Hid-induced apoptosis. We found an excess of AMPs in *Hid* mutants (Fig. 3H; Table 1), which demonstrates that Hid is the major component of the apoptotic pathway controlling AMP cell numbers. To further investigate the potential role of EGFR signalling in AMP cell survival, we focused on the lateral region and attempted to identify EGF-sending cells by monitoring *rho* expression. We did not find *rho* expression in PNS neurons (see Fig. S2 in the supplementary material). However, our data clearly show that in each hemisegment, one mesodermal cell corresponding to lateral oblique 1 (LO1) muscle founder (Fig. 3L,M; see Fig. S3, Movie 6 in the supplementary material) and several epidermal cells (Fig. 3N,O; see Movie 7 in the supplementary material) all express high levels of *rho* and are thus expected to secrete the EGF ligand Spitz. Consistent with these findings and with the concomitant accumulation of phospho-ERK in AMPs (see Fig. S4 in the supplementary material), the overexpression of *rho* in specified muscle founders (Fig. 3J) or in ectodermal cells (Fig. 3K) leads to an increased number of AMPs, similar to the pattern found in embryos deficient for apoptosis (Table 1). Taken together, our data show that EGFR signalling plays an active role in AMP cell specification and, in later stages, is reactivated in AMPs to protect them against apoptosis (Fig. 3I).

Regulatory modules operating in LAMPs

We have previously reported (Jagla et al., 1998) that *lb* homeobox genes are expressed in LAMPs and are required for their specification, suggesting that they might act as targets of the EGFR

Table 1. Number of Twist-labelled wild-type AMPs and different gain- and-loss-of-function mutant embryos

Genotype	VAMP	LAMP	DLAMP	DAMP
Wt	1.0 (±0.0)	2.3 (±0.5)	2.7 (±0.7)	1.0 (±0.2)
24B Gal4>EP3704 (*rho*)	1.4 (±0.5)	9.0 (±4.6)	8.0 (±4.3)	2.4 (±1.1)
Duf Gal4>EP3704 (*rho*)	1.0 (±0.1)	3.0 (±0.9)	3.6 (±0.6)	1.5 (±0.7)
69B Gal4>EP3704 (*rho*)	1.1 (±0.4)	3.4 (±1.1)	3.8 (±1.1)	2.4 (±1.1)
star (2772)	1.2 (±0.4)	0.5 (±0.7)	1.4 (±0.9)	1.1 (±0.5)
spitz1 (1859)	1.0 (±0.0)	1.3 (±1.0)	2.1 (±0.9)	1.5 (±1.0)
24B Gal4>EGFRCA (4846)	1.2 (±0.4)	10.5 (±4.2)	12.1 (±5.0)	6.4 (±3.1)
Twist Gal4>EGFRDN (5364)	1.0 (±0.0)	0.7 (±0.7)	1.2 (±0.9)	1.0 (±0.5)
24B Gal4>UAS Ras 85D (4847)	1.8 (±1.1)	11.6 (±3.6)	19.8 (±3.4)	5.5 (±2.0)
H99 (1576)	0.9 (±0.2)	4.2 (±1.5)	2.9 (±0.8)	1.2 (±0.6)
Hid A329	1.0 (±0.3)	3.1 (±1.6)	2.9 (±1.0)	2.2 (±1.2)

Values represent averages of 50 hemisegments with errors. Bloomington Stock Center reference numbers are indicated in brackets.

pathway. Interestingly, *lb* genes are also expressed in the neighbouring segment border muscle (SBM) muscle and are required for its fibre-type-specific differentiation (Jagla et al., 1998; Junion et al., 2007). This raises questions as to the regulatory modules that drive *lb* expression in differentiating SBM versus the regulatory modules allowing LAMP-specific expression. In order to identify the *lb* enhancers, we systematically tested non-coding sequences lying upstream and downstream of *lb* genes by *lacZ* reporter transgenesis (see Fig. S5 in the supplementary material). We started by testing, in vivo, 16 overlapping DNA fragments ranging from 1.2-4.5 kb. This lead us to the identification of epidermal, neural and mesodermal regulatory modules (see Fig. S5 in the supplementary material). They included a 2.1 kb fragment located 3.8 kb downstream to the *lbe* (*ladybird early*) gene that was found to drive expression in both mesodermal cell types, i.e. SBM and LAMPs, whereas a 1.5 kb fragment lying 11.1 kb upstream to the *lbe* transcription start site was able to drive expression in LAMPs only. Several constructs were then tested within these regions to identify minimal enhancers (Fig. 4A). A 560 bp sequence called LME (ladybird muscle enhancer), capable of driving *lacZ* expression in both SBM and LAMPs, was dissected from the initial 2.1 kb fragment. Importantly, the *LME-lacZ* line recapitulates all aspects of *lbe* expression in both SBM and LAMPs (Fig. 4B,C). We attempted to separate SBM and LAMP modules but failed to get *lacZ* transgenic lines displaying specific SBM-only or LAMP-only expression. Dissection of the upstream 1.5 kb fragment resulted in the identification of a 156 bp DNA module named LAMPE (lateral adult muscle precursor enhancer), which drives expression in LAMPs (Fig. 4D,E) in a similar manner to the 1.5 kb fragment. To understand how LME and LAMPE enhancers function and to determine whether they can act as transcriptional targets for effectors of EGFR signalling, we analyzed their sequences searching for evolutionarily conserved motifs and transcription factor binding sites, with special focus on the ETS sites to which EGFR effectors bind. We found that both enhancers carry potential ETS binding sites. Within the LME enhancer, in addition to an ETS site, there were two potential Lb binding sites and one Mef2 binding site that were found to be a part of the conserved sequence boxes (Fig. 5A), whereas the LAMPE element housed two perfectly conserved boxes carrying two potential ETS-binding sequences and three homeodomain-binding (Lb) motifs (Fig. 5A). To test whether the identified ETS binding sites are functional, we generated transgenic lines carrying disrupted ETS motifs (ETSmut). We observed that *lacZ* expression was specifically downregulated in the ETSmut LME line or lost in the ETSmut LAMPE line (Fig. 5J-M), demonstrating that ETS sites are essential for driving expression in LAMPs. As documented by ectopic *LAMPE-lacZ* expression in EGFR gain-of-function embryos (see Fig. S6 in the supplementary material), the identified motifs act as transcriptional targets of the EGFR pathway in vivo. The presence of homeodomain binding motifs within both LME and LAMPE elements also suggested that Lb itself is important for the activity of both enhancers. To test this, we generated a series of transgenic lines with disrupted homeodomain binding sites. We found that *lacZ* expression driven either by Lbmut LAMPE (Fig. 5I) or by Lbmut LME elements (data not shown) was no longer detected in *lb*-positive lineages. Further evidence of a key role of Lb autoregulation is the capacity of Lbe to induce LAMPE-driven *lacZ* expression in an increased number of mesodermal cells (see Fig. S6 in the supplementary material). Thus, the homeodomain-binding motifs appear crucial for both enhancers. As mentioned earlier, the LME element driving expression in differentiated SBM

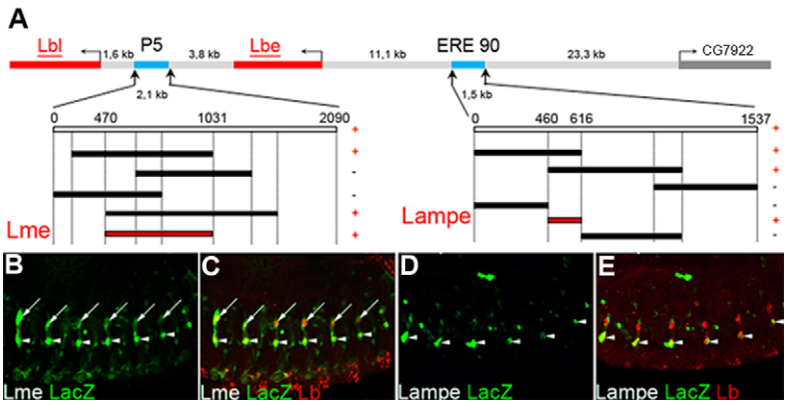

Fig. 4. Minimal *lb* enhancers driving expression in lateral AMPs and in differentiated SBM muscle. (**A**) (Upper) Scheme illustrating the location of mesodermal *lb* enhancers. (Lower) Schematic representation of the identification of minimal enhancers (*LME* within the P5 and *LAMPE* within ERE90 regions), showing the location of different sub-fragments tested in an in vivo *lacZ* reporter assay in transgenic *Drosophila* lines. Fragments found to drive *lacZ* expression in LAMPs and/or SBM lineage are flagged by a red '+' sign. Positions of LME and LAMPE minimal enhancers are indicated. (**B**,**C**) LME drives *lacZ* expression in *lb*-positive mesodermal lineages: LAMPs (arrowheads) and the SBM (arrows). (**D**,**E**) LAMPE-directed *lacZ* expression coincides with *lb* expression in LAMP cells (arrowheads).

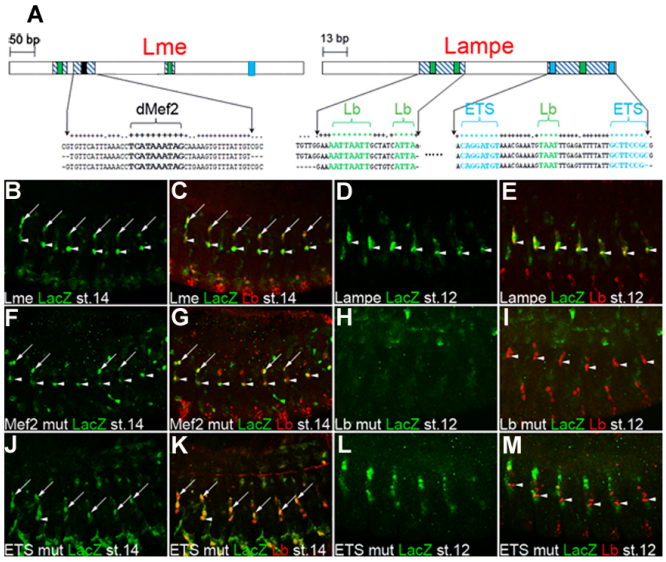

Fig. 5. Transcription factor binding sites required for the enhancer activities of LME and LAMPE. (**A**) Scheme showing distribution of Lbe/Hom (green boxes), ETS/Pointed (blue boxes) and Mef2 (black box) binding sites within LME and LAMPE. Sequence motifs conserved between *D. melanogaster*, *D. virilis* and *D. pseudobscura* are depicted as shaded boxes. Corresponding sequence alignments are shown below. (**B**,**C**) *LME-lacZ* expression in SBM (arrows) and in LAMPs (arrowheads). (**D**,**E**) LAMPE-driven *lacZ* expression in LAMPs (arrowheads). (**F**,**G**) Mutation of conserved Mef2 binding site within the LME enhancer leads to a partial loss of *lacZ* expression in SBM cells (arrows) but not in LAMPs (arrowheads). (**H**,**I**) Disrupting all three potential Lb binding sites resulted in a complete loss of LAMPE-driven *lacZ* expression. (**J**,**K**) Disruption of the ETS binding site results in partial loss of LME *lacZ* expression in LAMPs without affecting expression in SBM lineage (arrows). (**L**,**M**) Mutation of both of the conserved ETS binding sites within LAMPE leads to ectopic *lacZ* expression and loss of *lacZ* in LAMPs. Arrowheads in I and M point to Lb expression in LAMPs.

and undifferentiated LAMP cells carries a perfect Mef2 binding motif that is not present in the LAMPE enhancer driving expression in the LAMP lineage only. This prompted us to test whether the Mef2 site plays a role in the SBM-specific activity of LME. As shown in Fig. 5F and 5G, the majority of the SBM-specific expression of *lacZ* is lost in transgenic embryos carrying LME with a mutated Mef2 site, whereas *lacZ* expression in LAMPs remains unaffected.

Taken together, the in vivo analyses of LME and LAMPE regulatory modules reveal a pivotal role of ETS binding sites and EGFR signalling in driving AMP-specific expression, and a key role for the Mef2 binding site in driving expression in differentiating muscle cells.

DISCUSSION

Understanding how different populations of stem cells are specified, how they maintain their undifferentiated state during development and, from there on, how they are activated to enter differentiation is of prime importance for further progress in regenerative biology. One of the future challenges is to develop new animal models and tools making it possible to follow stem cells in vivo. Recent studies performed in the fruit fly have led to the identification of several stem cell populations (for a review, see Pearson et al., 2009), making *Drosophila* an attractive model system for stem cell biology that is well adapted to in vivo approaches. Here, we exploit the amenability of the *Drosophila* system to gain insights into the specification and behaviour of AMPs, which emerge as a novel population of muscle-committed transient stem cells in *Drosophila*.

Repressors of myogenic differentiation and targets of the Notch pathway are specifically expressed in AMPs

It has been previously reported (Ruiz Gomez and Bate, 1997) that a subset of muscle progenitors divides asymmetrically and gives rise to *numb*-positive founder cells that undergo differentiation and to *Notch*-expressing AMPs. Through this pathway, six AMPs are born in each abdominal hemisegment. In contrast to founders, AMPs express the Notch target Him (Rebeiz et al., 2002; Liotta et al., 2007) and *Zfh1*, the *Drosophila* homolog of *ZEB* (27), both of which are able to counteract Mef2-driven myogenic differentiation. Interestingly, another general AMP marker, E(spl)M6, also corresponds to a Notch target (Rebeiz et al., 2002), suggesting that Notch signalling could play an evolutionarily conserved role in muscle cell stemness. It operates not only in vertebrate satellite cells (Conboy and Rando, 2002; Vasyutina et al., 2007; Carlson et al., 2008) but also, as we show here, in *Drosophila* AMPs. Finally, we report that, similar to muscle progenitors, the AMPs are heterogenous and express different muscle identity genes, such as *lb or slou* (Jagla et al., 1998; Knirr et al., 1999). This strongly suggests that AMPs acquire a positional identity that makes them competent to form a given type of muscles during adult myogenesis. For example, the lateral AMPs expressing *lb* are at the origin of all lateral body wall muscles of the adult fly. In support of the specific positional identities of AMPs comes also the analysis of *lame duck* (*lmd*) mutant embryos known to be devoid of fusion-competent myoblasts (FCMs) (Sellin et al., 2009). In this mutant context, the number of Twi-positive and Zfh1-positive AMP-like cells is highly increased, while the number of Lbe- and Twi-positive LAMPs committed to the lateral lineage remains unchanged (Sellin et al., 2009). Thus in the absence of *lmd*, some presumptive FCMs can adopt the AMP-like fate but they do not carry positional information transmitted by the identity genes such as *lb*.

Embryonic AMPs form a network of interconnected cells

Based on the premise that the AMPs correspond to a novel population of transient stem cells, we attempted to analyze their shapes and behaviour in living embryos carrying M6-GAL4 and UAS-GAP-GFP transgenes. To our surprise, we found that shortly after their specification, the AMPs start to send cellular processes that align along the nerves of the PNS, with the result that, by the end of embryogenesis, all AMPs become linked together. Interestingly, the intersegmental connections are made via an intermediary M6+ twi– cell of unknown fate. In addition to this particular cell, which ensures the intersegmental link between AMPs, the embryos also contained other M6+ twi– non-neural cells of rounded morphology located more internally that were unconnected to the AMP cell network. The origin and identity of these cells remain unknown.

Exploiting the possibility of following AMPs in vivo, we tested how AMPs would behave if we broke their connections. As the AMPs separated from the network by laser ablation changed shape

and lost their normal positions, we concluded that one important reason for which AMPs form a cell network is to keep precise spatial positioning. Based on the observation that AMPs send long cellular processes along the peripheral nerves, it is probable that nerves serve as a support for extending AMP cell protrusion. This possibility is supported by the abnormal pattern of AMPs observed in *daughterless* mutant embryos (Bate et al., 1991) lacking the PNS and in embryos in which the PNS was affected by the Elav-GAL4 driven expression of the inducer of apoptosis, Reaper (data not shown). PNS nerves might also represent a source of signals for AMPs such as Delta in order to maintain Notch activity. However, analysis of the lateral domain revealed that *Delta* expression was associated with the SBM precursor but not with the PNS neurons (see Fig. S7 in the supplementary material), indicating that Notch activity in lateral AMPs is regulated by Delta produced in the SBM rather than in nerves (see Fig. 6).

EGF signalling is required for specification and maintenance of AMPs in embryos

Taking advantage from the restricted number of embryonic AMPs and the genetic tools available in *Drosophila*, we performed a large-scale gain-of-function screen to identify the genes involved in AMP specification. We found that *rho* and other components of the EGF signalling pathway are crucially required for both specification and maintenance of AMPs. Importantly, as reported by Krejci et al. (Krejci et al., 2009), several components of EGF signalling are direct targets of Notch in AMPs, thus creating a link between the two signalling pathways. The high number of AMPs in EGFRCA and RAS gain-of-function contexts provides evidence that RAS signalling not only promotes muscle founder specification, as reported previously (Artero et al., 2003), but is also crucial for specifying AMPs when induced by EGF signals.

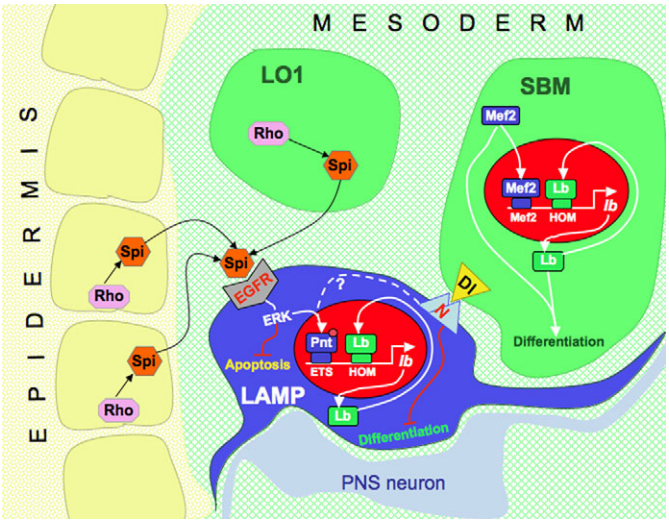

Fig. 6. Scheme illustrating regulatory modules and regulatory inputs operating in non-differentiated (LAMP) and differentiated (SBM) muscle cells. Laterally located AMP (blue) requires the EGFR pathway for its specification and maintenance. The activity of LAMP-specific regulatory modules depends on extrinsic EGF signals emitted by the mesodermal LO1 founder and the neighbouring epidermal cells. LAMP also displays Notch activity, most probably activated via Delta emitted by the SBM precursor. By contrast, the regulatory element operating in differentiated SBM muscle lineage appears independent of extrinsic influence. It is positively regulated by intrinsic Mef2 and maintained active via an *lb* autoregulatory feedback loop.

Further support for a key role of the EGFR pathway is the identification of cells sending EGF to lateral AMPs and the demonstration of their role in AMP cell maintenance (Fig. 6). It also turns out that the anti-apoptotic role of the EGFR pathway in *Drosophila* AMPs described here is conserved across evolution, as EGF signalling also promotes survival of vertebrate satellite cells (Golding et al., 2007).

Conserved EGF-response element is required to drive *lb* expression in LAMPs

The evidence for a major role of the EGFR pathway in the specification and maintenance of AMPs raises important questions about EGF targets operating in these muscle-committed stem-like cells in *Drosophila*. We have previously demonstrated that *lb* genes are required for specification of LAMPs (Jagla et al., 1998), making them candidate targets of EGF signalling in the lateral region. Here, we show that *lb* regulatory modules contain binding sites for ETS factors that act as EGFR effectors and go on to demonstrate their crucial role in AMP enhancer activity. The proximity of the ETS binding sites and homeodomain binding sites in the AMP element suggests that an adapted spatial conformation of interacting factors is important in allowing simultaneous binding and thus maintenance of the lineage-restricted activity of this enhancer. Interestingly, the main difference between regulatory modules driving expression in differentiated muscle lineages versus regulatory modules that act in non-differentiated AMPs is the responsiveness of the latter category to extrinsic EGF signals. In opposition to this (Fig. 6), we found that intrinsic Mef2 inputs are sufficient to drive expression in differentiated muscle lineage. The ETS and Mef2-driven expression of these two distinct regulatory modules is positively regulated by *lb*, which is known to play a pivotal role in the specification of muscle lineages in the lateral domain. The specific expression of *lb* in a subset of AMP cells and of its ortholog *Lbx1* in activated satellite cells (Watanabe et al., 2007) suggests that similarities in genetic control of *Drosophila* and vertebrate muscle stem cells might extend beyond those discussed here.

Acknowledgements
This work was supported by the Institut National de la Santé et de la Recherche Médicale, the Association Française contre les Myopathies, the Association pour la Recherche sur le Cancer, the Fondation pour la Recherche Médicale and European Grant LSHG-CT-2004-511978 to the MYORES Network of Excellence.

Competing interests statement
The authors declare no competing financial interests.

Supplementary material
Supplementary material for this article is available at
http://dev.biologists.org/lookup/suppl/doi:10.1242/dev.049080/-/DC1

References
Artero, R., Furlong, E. E., Beckett, K., Scott, M. P. and Baylies, M. (2003). Notch and Ras signaling pathway effector genes expressed in fusion competent and founder cells during *Drosophila* myogenesis. *Development* **130**, 6257-6272.
Bate, M., Rushton, E. and Currie, D. A. (1991). Cells with persistent twist expression are the embryonic precursors of adult muscles in Drosophila. *Development* **113**, 79-89.
Bergmann, A., Tugentman, M., Shilo, B. Z. and Steller, H. (2002). Regulation of cell number by MAPK-dependent control of apoptosis: a mechanism for trophic survival signaling. *Dev. Cell* **2**, 159-170.
Bidet, Y., Jagla, T., Da Ponte, J. P., Dastugue, B. and Jagla, K. (2003). Modifiers of muscle and heart cell fate specification identified by gain-of-function screen in *Drosophila*. *Mech. Dev.* **120**, 991-1007.
Bodmer, R., Barbel, S., Sheperd, S., Jack, J. W., Jan, L. Y. and Jan, Y. N. (1987). Transformation of sensory organs by mutations of the cut locus of *D. melanogaster*. *Cell* **51**, 293-307.

Carlson, M. E., Hsu, M. and Conboy, I. M. (2008). Imbalance between pSmad3 and Notch induces CDK inhibitors in old muscle stem cells. *Nature* **454**, 528-532.
Conboy, I. M. and Rando, T. A. (2002). The regulation of Notch signaling controls satellite cell activation and cell fate determination in postnatal myogenesis. *Dev. Cell* **3**, 397-409.
Duan, H., Zhang, C., Chen, J., Sink, H., Frei, E. and Noll, M. (2007). A key role of Pox meso in somatic myogenesis of *Drosophila*. *Development* **134**, 3985-3997.
Farrell, E. R. and Keshishian, H. (1999). Laser ablation of persistent twist cells in *Drosophila*: muscle precursor fate is not segmentally restricted. *Development* **126**, 273-280.
Figeac, N., Daczewska, M., Marcelle, C. and Jagla, K. (2007). Muscle stem cells and model systems for their investigation. *Dev. Dyn.* **236**, 3332-3342.
Golding, J. P., Calderbank, E., Partridge, T. A. and Beauchamp, J. R. (2007). Skeletal muscle stem cells express anti-apoptotic ErbB receptors during activation from quiescence. *Exp. Cell Res.* **313**, 341-356.
Jagla, T., Bellard, F., Lutz, Y., Dretzen, G., Bellard, M. and Jagla, K. (1998). Ladybird determines cell fate decisions during diversification of *Drosophila* somatic muscles. *Development* **125**, 3699-3708.
Junion, G., Jagla, T., Duplant, S., Tapin, R., Da Ponte, J. P. and Jagla, K. (2005). Mapping Dmef2-binding regulatory modules by using a ChIP-enriched in silico targets approach. *Proc. Natl. Acad. Sci. USA* **102**, 18479-18484.
Junion, G., Bataillé, L., Jagla, T., Da Ponte, J. P., Tapin, R. and Jagla, K. (2007). Genome-wide view of cell fate specification: ladybird acts at multiple levels during diversification of muscle and heart precursors. *Genes Dev.* **21**, 3163-3180.
Knirr, S., Azpiazu, N. and Frasch, M. (1999). The role of the NK-homeobox gene slouch (S59) in somatic muscle patterning. *Development* **126**, 4525-4535.
Krejci, A., Bernard, F., Housden, B. E., Collins, S. and Bray, S. J. (2009). Direct response to Notch activation: signaling crosstalk and incoherent logic. *Sci. Signal.* **2**, ra1.
Lai, E. C., Bodner, R. and Posakony, J. W. (2000). The enhancer of split complex of *Drosophila* includes four Notch-regulated members of the bearded gene family. *Development* **127**, 3441-3455.
Liotta, D., Han, J., Elgar, S., Garvey, C., Han, Z. and Taylor, M. V. (2007). The Him gene reveals a balance of inputs controlling muscle differentiation in *Drosophila*. *Curr. Biol.* **17**, 1409-1413.
Maqbool, T. and Jagla, K. (2007). Genetic control of muscle development: learning from *Drosophila*. *J. Muscle Res. Cell Motil.* **28**, 397-407.
Micchelli, C. A. and Perrimon, N. (2006). Evidence that stem cells reside in the adult *Drosophila* midgut epithelium. *Nature* **439**, 475-479.
Nagaso, H., Murata, T., Day, N. and Yokoyama, K. K. (2001). Simultaneous detection of RNA and protein by in situ hybridization and immunological staining. *J. Histochem. Cytochem.* **49**, 1177-1182.
Ohlstein, B. and Spradling, A. (2006). The adult *Drosophila* posterior midgut is maintained by pluripotent stem cells. *Nature* **439**, 470-474.
Pearson, J., López-Onieva, L., Rojas-Ríos, P. and González-Reyes, A. (2009). Recent advances in *Drosophila* stem cell biology. *Int. J. Dev. Biol.* **53**, 1329-1339.
Postigo, A. A., Ward, E., Skeath, J. B. and Dean, D. C. (1999). zfh-1, the *Drosophila* homologue of ZEB, is a transcriptional repressor that regulates somatic myogenesis. *Mol. Cell. Biol.* **19**, 7255-7263.
Rebeiz, M., Reeves, N. L. and Posakony, J. W. (2002). SCORE: a computational approach to the identification of cis-regulatory modules and target genes in whole-genome sequence data. Site clustering over random expectation. *Proc. Natl. Acad. Sci. USA* **99**, 9888-9893.
Ruiz Gómez, M. and Bate, M. (1997). Segregation of my
ogenic lineages in *Drosophila* requires numb. *Development* **124**, 4857-4866.
Sellin, J., Drechsler, M., Nguyen, H. T. and Paululat, A. (2009). Antagonistic function of Lmd and Zfh1 fine tunes cell fate decisions in the Twi and Tin positive mesoderm of *Drosophila melanogaster*. *Dev. Biol*. **326**, 444-455.
Sharma, Y., Cheung, U., Larsen, E. W. and Eberl, D. F. (2002). PPTGAL, a convenient Gal4 P-element vector for testing expression of enhancer fragments in *Drosophila*. *Genesis* **34**, 115-118.
Soler, C., Daczewska, M., Da Ponte, J. P., Dastugue, B. and Jagla, K. (2006). Coordinated development of muscles and tendons of the *Drosophila* leg. *Development* **131**, 6041-6051.
Spradling, A., Drummond-Barbosa, D. and Kai, T. (2001). Stem cells find their niche. *Nature* **414**, 98-104.
Sudarsan, V., Anant, S., Guptan, P., VijayRaghavan, K. and Skaer, H. (2001). Myoblast diversification and ectodermal signaling in Drosophila. *Dev. Cell* **1**, 829-839.
Takashima, S., Mkrtchyan, M., Younossi-Hartenstein, A., Merriam, J. R. and Hartenstein, V. (2008). The behaviour of *Drosophila* adult hindgut stem cells is controlled by Wnt and Hh signalling. *Nature* **454**, 651-655.
Vasyutina, E., Lenhard, D. C., Wende, H., Erdmann, B., Epstein, J. A. and Birchmeier, C. (2007). RBP-J (Rbpsuh) is essential to maintain muscle progenitor cells and to generate satellite cells. *Proc. Natl. Acad. Sci. USA* **104**, 4443-4448.
Watanabe, S., Kondo, S., Hayasaka, M. and Hanaoka, K. (2007). Functional analysis of homeodomain-containing transcription factor Lbx1 in satellite cells of mouse skeletal muscle. *J. Cell Sci.* **120**, 4178-4187.
Yu, F., Kuo, C. T. and Jan, Y. N. (2006). *Drosophila* neuroblast asymmetric cell division: recent advances and implications for stem cell biology. *Neuron* **51**, 13-20.